

# UNCLASSIFIED

AD NUMBER
AD062243
NEW LIMITATION CHANGE
TO Approved for public release, distribution unlimited
FROM Distribution authorized to U.S. Gov't. agencies and their contractors; Administrative/Operational Use; MAY 1955. Other requests shall be referred to Office of Naval Research, One Liberty Center, 875 North Randolph Street, Arlington, VA 22203-1995.
AUTHORITY
ONR ltr, 26 Oct 1977

THIS PAGE IS UNCLASSIFIED

AD 062243

Technical Report EXP-1-P

PROJECT SQUID

A COOPERATIVE PROGRAM  
OF FUNDAMENTAL RESEARCH  
AS RELATED TO JET PROPULSION  
FOR THE

OFFICE OF NAVAL RESEARCH, DEPARTMENT OF THE NAVY  
OFFICE OF SCIENTIFIC RESEARCH, DEPARTMENT OF THE AIR FORCE  
AND THE  
OFFICE OF ORDNANCE RESEARCH, DEPARTMENT OF THE ARMY

Contract N6-ori-105, Task Order III, NR-098-038

STUDIES OF IONIZATION IN FLAMES BY MEANS OF LANGMUIR PROBES

by

H. F. Calcote and I. R. King  
Experiment Incorporated  
Richmond 2, Virginia  
May 1955

PROJECT SQUID HEADQUARTERS  
JAMES FORRESTAL RESEARCH CENTER  
PRINCETON UNIVERSITY  
PRINCETON, N. J.

This paper was presented at the Fifth Symposium (International) on Combustion (Combustion in Engines and Combustion Kinetics) at Pittsburgh, Pennsylvania in September 1954. It will appear in the Fifth Combustion Symposium Volume to be published by the Reinhold Publishing Corporation sometime in 1955.

# STUDIES OF IONIZATION IN FLAMES BY MEANS OF LANGMUIR PROBES

By H. F. CALCOTE and I. R. KING<sup>1</sup>

## ABSTRACT

The use of the Langmuir probe in studying ionization in flames is described with typical results and an interpretation of some of the experimental evidence to prove that ionization in the combustion zone is not due to contaminants. The arguments for this conclusion are:

1. Flames of some fuels do not contain ions. Were contaminants responsible, all flames would be expected to have ions present.
2. Flames at low temperatures have high ion concentrations such that it would require one mole-percent sodium impurity in the input gas to account for the observed concentration.
3. Ionization is concentrated in a very thin region comparable in thickness to the reaction zone.
4. Results at different pressures can not be correlated by assuming thermal ionization of contaminants.

## Introduction

In previous publications (1) the concentration of positive ions in the combustion zone of a hydrocarbon flame has been estimated to be some  $10^{12}$  ions/cc. This estimate was obtained both by deflection of the flame in an electric field and by the increase in flame pressure when an electric field

---

<sup>1</sup> Experiment Incorporated, Richmond, Virginia.

is applied to the flame. This concentration is considerably greater than can be readily accounted for by thermal ionization of the species which are known to be present. It was therefore proposed that ions are produced, not by thermal processes, but by chemi-ionization or events similar to those causing abnormal electronic excitation in flames. The results have also been taken as evidence that thermal equilibrium does not exist between species in the flame front.

Further investigation of ions in the flame front has been carried out with small electric probes of the type developed by Langmuir (3) to study the properties of the electron plasma in electric discharges. Measurements of the attenuation of electromagnetic waves (4, 5) are inadequate for studies in the combustion zone since the region of reaction is only a fraction of a millimeter thick, whereas the wave length for short electromagnetic waves is approximately a centimeter. For this reason the probe technique was chosen in spite of the difficulties and limitations involved in placing a small probe into a high-temperature combustion zone.

Were ions due to thermal effects, that is, if they were in thermodynamic equilibrium with their parent species, it should be possible to calculate the ion concentration by means of Saha's relation (6, 7):

$$\log \frac{N_- N_+}{N_0} = \log K_N = \log G + 15.38 + \frac{3}{2} \log T - \frac{5040}{T} V_i \quad (1)$$

where  $K_N$  is the equilibrium constant for  $\underline{M} \rightleftharpoons \underline{M}^+ + \underline{e}^-$ ;  $N_-$ ,  $N_+$ , and  $N_0$  are the concentrations of electrons, positive ions, and neutral molecules per cubic centimeter;  $G = \underline{g}_- \underline{g}_+ / \underline{g}_0$ , and the  $\underline{g}$ 's are the statistical weights;  $T$  is the absolute temperature; and  $V_i$  is ionization potential in electron volts. The contributions of various species to the thermal ionization in a

propane-air flame are presented in table 1. The equilibrium concentrations of the species at the stoichiometric adiabatic flame temperature,  $T_b$ , are tabulated in the third column and were employed as  $N_0$  in equation (1) to calculate the theoretical ion concentration at 2200°K, and at 1400°K. The last column corresponds to a lean flame with a low flame temperature and the same concentrations of neutral species as might exist in a stoichiometric flame. The only real possibilities for ion sources in this set of products are nitric oxide, graphitic carbon (5, 8), and the contaminant sodium (9) or other alkali metal. Actually, in the low-temperature flame graphitic carbon would be the only real contender, and this calculation is based upon the work function for graphite (4.35 e.v.) instead of that for a small carbon particle with an ionization potential of 8.5 e.v. as suggested by Shuler (5). Employing for the equivalent concentration of carbon atoms  $N_0 = 4.2 \times 10^{13}$  from table 1, the ion concentration arising from carbon is 36 ions/cc in the 1400°K flame. Experimental ion concentrations in lean flames where the temperature is low would thus be useful in considering possible sources of ions. Such data have therefore been obtained in the present program.

This paper outlines the probe technique, with typical results, and presents experimental evidence that ionization in the combustion zone is not due to contaminants.

#### I. Absolute Reaction Rate Theory of the Langmuir Probe

If a wire (probe) be placed in an ionized plasma and the current to this probe plotted as a function of the applied voltage, a curve such as that presented in figure 1 is obtained. When the probe is strongly negative with respect to the plasma, only positive ions will reach it; electrons are repelled as they approach. Only electrons and positive ions are considered because it has been well established that the negative species in flames are mainly electrons (10). As the probe potential becomes less negative, the fastest

electrons will reach the probe, decreasing the total current. The ionic and electronic currents will balance at some negative probe potential because the electrons have a higher mobility than do the positive ions. This probe voltage is called the wall potential. A further increase in probe voltage causes the electron current to exceed the ionic current. The analysis of curves such as figure 1 by Langmuir Probe Theory permits one to draw a number of conclusions concerning the nature of the plasma.

Although the theory of the Langmuir probe is described in a number of places (3, 11), it is instructive to derive it by applying the theory of absolute reaction rates (2) to the process. This is a fresh approach and should help to make the phenomena more readily understood. According to the theory of absolute reaction rates, any rate process can be described by the following (12):

$$\text{RATE} = \kappa N^{\ddagger} \frac{kT}{h} \quad (2)$$

where  $\kappa$  is a transmission coefficient, usually equal to one. The concentration of activated species (or complex) at the top of a potential-energy barrier limiting the rate process is  $N^{\ddagger}$ . The universal frequency factor  $kT/h$  represents the frequency with which the activated species crosses the barrier at a given temperature,  $T$ ;  $k$  is the Boltzmann constant and  $h$  is Planck's constant. Applying this relation to the rate at which electrons reach the negative probe, one obtains for the electron current per unit area,  $j_-$ ,

$$j_- = \kappa e N^{\ddagger} \frac{kT_-}{h} \quad (3)$$

The activated electrons,  $N_-^{\ddagger}$ , which have overcome the probe potential (fig. 2) are multiplied by  $e$ , the electronic charge, to obtain the current. The electron temperature is  $T_-$ , assuming a Maxwell-Boltzmann velocity distribution among the electrons. The activated electron concentration,  $N_-^{\ddagger}$  can be written in terms of an equilibrium constant between electrons in the plasma and on the probe surface,

$$\frac{N_-^{\ddagger}}{N_-} = K^{\ddagger} = \frac{{}^0F_-^{\ddagger}}{{}^0F_-} \quad (4)$$

where  ${}^0F_-$  is the partition function for electrons per unit volume in the plasma, and  ${}^0F_-^{\ddagger}$  is per unit area since only two degrees of freedom are available for activated electrons on the probe surface. Equation (3) is then written, assuming  $K^{\ddagger} = 1$ , as

$$j_- = e N_- \frac{{}^0F_-^{\ddagger}}{{}^0F_-} \frac{kT_-}{h}$$

When the energy difference,  $eV$ , between electrons in the plasma and on the probe surface is written explicitly, this equation becomes

$$j_- = \frac{kT_-}{h} e N_- \frac{F_-^{\ddagger}}{F_-} e^{-eV/kT_-}$$

Writing out the partition functions, which involve only translational degrees of freedom, the following is obtained:



$$j_- = \frac{kT_-}{h} eN_- \frac{2\pi m_- kT_- / h^2}{(2\pi m_- kT_- / h^2)^{3/2}} e^{-eV/kT_-}$$

where  $m_-$  is the mass of an electron. This equation reduces to

$$j_- = eN_- \sqrt{\frac{kT_-}{2\pi m_-}} e^{-eV/kT_-} \quad (5)$$

Equation (5) can be rewritten,

$$\ln j_- = B - \frac{eV}{kT_-} \quad (6)$$

A plot of  $\ln j_-$  against  $V$  gives a means of evaluating the electron temperature,  $T_-$ . The intercept gives the constant  $B$ , which can be employed to evaluate  $N_-$ .

For positive ions there will be an equation similar to (5), but with a negative probe the exponent will effectively equal one. A space charge will form around the probe, the thickness of which will vary with the probe voltage. This causes the effective probe area to change. All ions entering the charged region will be captured by the probe, that is, the current will be space-charge limited. Thus,

$$N_+ = \frac{j_+}{e} \sqrt{\frac{2\pi m_+}{kT_+}} \quad (7)$$

The positive-ion temperature,  $T_+$ , must be very near the gas temperature, so that if one assumes or knows  $m_+$ , equation (7) permits a calculation of the concentration of positive ions. In an undisturbed plasma  $N_+ = N_-$ ; in a small flame, however, it is possible that the higher diffusion rate of electrons may permit them to diffuse out of the plasma, causing  $N_+$  to exceed  $N_-$ .

The wall potential,  $V_w$ , can be easily derived since here the probe current  $j_p = j_+ - j_- = 0$ . Then from equations (5) and (7),

$$V_w = \frac{kT_-}{2e} \ln \frac{T_- m_+}{T_+ m_-} \quad (8)$$

provided  $N_-$  be indeed equal to  $N_+$ . This relation should permit a calculation of  $T_+$  or  $m_+$ , depending upon which is known or can be reasonably assumed.

This brief outline of Langmuir Probe theory will suffice for present purposes. For a more detailed discussion covering difficulties involved in applying the theory and considerations of the thickness of the ion sheath surrounding the probe, the reader is referred to Loeb (11).

## II. Experimental Determination of Ion Concentration

The positive-ion concentration through the combustion wave was obtained by constructing Langmuir probe curves (fig. 1) at a series of closely spaced points through the flame front. The positive-ion current,  $i_+$ , was then obtained as indicated in figure 1 and plotted against the probe movement (fig. 3). The slope of this curve at any given point gave the positive-ion concentration at the given point. From this information curves like figure

4 were plotted. Distance was measured from the position where the probe first showed a bright red tip.

Considering figure 3, the total current to the probe will be given by

$$i_+ = 2\pi r \int_0^x j_+ dx \quad (9)$$

where  $r$  is the probe radius and  $x$  is the length of the probe in the ionized region. Differentiation yields

$$j_+ = \frac{1}{2\pi r} \frac{di_+}{dx}$$

The derivative  $di_+/dx$  is the slope of the curve in figure 3. Combining this relation with equation (7) the positive-ion concentration is obtained,

$$N_+ = \frac{di_+/dx}{2\pi er} \sqrt{\frac{2\pi m_+}{k T_+}}$$

or,

$$N_+ = \text{constant} \frac{(di_+/dx)}{r} \sqrt{\frac{m_+}{T_+}} \quad (10)$$

Thus, if a value be assumed for the mass of the positive ion and the positive-ion temperature be assumed equal to the adiabatic flame temperature, it is possible to determine the positive-ion concentration at any point in the flame. For all of the experiments reported here, except when salts have been added, the mass of the positive ion has been assumed to be  $3.3 \times 10^{-23}$  grams, corresponding to a molecular weight of 20.

The electrical circuitry (figs. 5 and 6) includes a means of measuring the electrical current to a sample probe as a function of the applied probe potential. A synchronous motor (3 RPM) is used to drive a variable resistance, thus varying the voltage as a function of time so that the recording current-time meter actually records current voltage. Since the instrument used for the current measurements must not only be extremely sensitive but must also have a low input resistance, a Millivac MR-61A micromicroammeter with a Sanborn Recorder was selected. Shielding was used wherever possible to prevent stray pickup. The probe was connected to the recorder by Teflon-insulated coaxial cable to reduce electrical leakage. The possibility of contact potentials was of course ever present. Thermionic emission has been calculated to be some 1000 times less than the observed current at the probe temperature of 1500°K. A series of preliminary experiments on the effect of probe diameter and of material for nichrome, platinum, and platinum-40-percent rhodium probes indicated that the experimental results are independent of probe size or material within the experimental error.

The type of flame to be probed was determined by several stringent conditions. First, it was desirable that the probe enter the flame front at right angles and that the exact position of the probe with respect to the flame front be known at all times. Secondly, since the probe itself must be extremely small, it was imperative that the probe enter the flame front from the cool side.

In order to satisfy the above conditions a 3.5-inch I. D. flat-flame burner was constructed (fig. 6). Fine-mesh screen wire was used to maintain laminar flow. A water jacket was installed around the burner port to maintain a constant temperature. The large flat flame has a great advantage over conventional Bunsen flames in that much leaner mixtures, with lower flame temperatures, can be burned. This permits the use of probes which would

deteriorate in a high-temperature flame. The probe entered the burner from the bottom, passed through a 1/4-inch tapered stainless-steel guide tube, and entered the flame from the cool or downstream side. The probe was driven manually through the flame front by means of a micrometer. Other types of flames were sometimes employed and will be described when referred to.

### III. Ionization in Flames Containing Alkali Chlorides

As a means of examining the probe technique flames were studied into which a known concentration of alkali chlorides had been introduced and the experimental results were compared with the theoretical ion concentrations predicted thermodynamically by Saha's equation.

The burner shown in figure 7 was used to introduce salt solutions into a Meker-type flame. A 500-ml round-bottom flask served as the spray chamber with the neck serving as the solution tube. A one-inch O.D. glass tube 21 inches long served as the burner. The burner tube was made long to allow any of the larger droplets entering the gas stream to fall back before entering the flame. In this way only a very fine mist entered the flame. The salt concentration in the gas stream was determined by measuring the change in solution height with time. No measurements were made until the burner had been in operation for several minutes so that equilibrium was attained between the salt solution entering the flame and the salt solution condensing on the walls and running back into the solution tube. The measurements were made over a 45-minute period. The feed rate was adjusted by regulating the needle valve controlling the quantity of gas passing through the sprayer. Reasonable changes in the liquid feed rate caused insignificant alterations of the theoretical atom concentration; for example, changing the liquid feed rate from 0.0050 to 0.0060 cc/sec changed the sodium-atom concentra-

tion in the flame from  $1.32$  to  $1.58 \times 10^{15}$  atoms/cc or the thermodynamic sodium-ion concentration from  $5.92$  to  $6.25 \times 10^{10}$  ions/cc. In computing the positive-ion concentration in the flame the concentration in the unburned gas was corrected for temperature rise but was not corrected for changes in the total number of molecules.

The electrical setup (fig. 7) was essentially the same as that used in flat-flame measurements with the exception that the probe position was fixed in the flame. A screen was suspended over the flame and grounded to give more consistent results by better fixing the ion plasma potential of the flame. A screen was suspended over the flame and grounded to give more consistent results by better fixing the ion plasma potential of the flame. The probe was located  $0.7$  cm above the burner grid and protruded approximately  $1.5$  cm into the flame. The actual position of the probe with respect to the burner was held constant in all experiments. Vertical movements up to one cm made no observable changes in current. The probe curve was obtained by averaging more than 5 Langmuir probe curves for each test. The difference between curves was negligible; for example, in experiment no. 7 (9 curves) the standard deviation of the positive-ion current about the arithmetic mean of  $5.21 \times 10^{-6}$  amperes was  $0.19 \times 10^{-6}$  amperes.

Probe length was determined by holding a vernier caliper near the probe. Half way between the points of a dull color and bright white ( $<0.2$  cm) was taken as the point of entrance of the probe into the flame. Changing the assumed probe length from  $1.4$  to  $1.6$  cm for CsCl changed the apparent ion concentration from  $2.86$  to  $2.51 \times 10^{10}$  ions/cc, an insignificant change.

The day-to-day reproducibility was extremely good; for example, with a 0.10 M NaCl solution giving  $1.96 \times 10^{14}$  sodium atoms/cc in the flame the experimental ion concentrations were

	<u>Date</u>	<u>Ion Concentration</u>
Same Mixture	30 Dec 53	$12.2 \times 10^8$ ions/cc
	7 Jan 54	11.6
New Mixture	7 Jan 54	11.9

The results of experiments with alkali chlorides added to the flame are summarized in table 2. The theoretical positive-ion concentration is some 400 times greater than the experimental result. The cause of this discrepancy is probably the cooling effect of the large probe. The temperature of the probe was determined with an optical pyrometer and found to be approximately 1400°K (column 5, table 2). If it be assumed that the probe cools the surrounding gas so that the effective temperature is 1500°K, the correlation of experimental and theoretical values is as indicated in table 2 and figure 8. Apart from the reasonableness of assuming a temperature slightly in excess of the probe temperature, the value 1500°K receives support from the fact that the agreement between theory and experiment is now reasonably good with respect to changing the alkali metal or the concentration of the salt (see table 2). For sodium the experimental-to-theoretical ion-concentration ratio is greater than for the other alkali metals. A similar discrepancy has also been noted by Wilson (10) using the conductivity method and by Belcher and Sugden (4) using the electromagnetic attenuation method for determining electron concentration. The cause of this discrepancy is unknown.

From figure 8 and table 2 it can be concluded, if it be assumed that the ion plasma being sampled has been cooled, that the probe samples the ion concentration fairly well, although the slopes of the experimental and theoretical lines in figure 8 are somewhat different. It would therefore be reasonable in interpreting probe results in flames to assume that the relative values obtained are comparable and that the absolute concentrations are some 400 times greater than the experimental result. Fortunately this error is on the conservative side for the arguments which are to be formulated from the data presented in the remainder of this paper. None of the results have been corrected except where indicated.

#### IV. Flames Containing Negligible Ionization

Because the presence of a minute quantity of alkali metal in the atmosphere would give ion concentrations of the order which have been measured, it is necessary to investigate this possibility further. Actually, to obtain  $10^9$  ions/cc at  $2300^\circ\text{K}$  by Saha's equation (see equation 1) requires only  $4.2 \times 10^9$  sodium atoms/cc or  $1.7 \times 10^{-8}$  mole-percent sodium. Since this concentration is well below that which would be amenable to ordinary analytical techniques, the concentration of interfering contaminants will have to be inferred. Thus, if a flame could be found in which the ion concentration were extremely small -- where the expected impurities were just as great as in a propane-air flame -- it might be argued that the ionization in the propane-air flame is a property of the flame and not due to impurities.

In connection with this line of reasoning it was found that neither a hydrogen sulfide-air flame (flame temperatures up to  $2100^\circ\text{K}$ ) nor a carbon disulfide-air flame (flame temperature between  $1625^\circ$  and  $2265^\circ\text{K}$ ) contained



ion concentrations within the limits of measurement. For carbon disulfide, stored in glass bottles, it might be expected that sodium would leach out of the glass. The air supply was of course the same as supplied the propane-air flames. In a specific experiment with a carbon disulfide-air flame on a Meker burner at an equivalence ratio ( $\phi$ ) of 0.85 ( $\phi$  = stoichiometric air-fuel ratio divided by the actual air-fuel ratio) the following were observed:

Adiabatic flame temperature,  $T_b = 2070^\circ\text{K}$

Probe temperature,  $T_p = 1255^\circ\text{K}$

Probe length = 1.6 cm, diameter = 0.063 cm

Positive-ion current,  $i_+$  =  $0.3 \times 10^{-9}$  amperes

Positive-ion concentration,  $N_+$  =  $2.2 \times 10^{-5}$  ions/cc

The result for  $i_+$  and  $N_+$  is only approximate because the sensitivity of the detecting instrument had to be set so high that electrical noise became appreciable.

Since it has been demonstrated that flames exist which possess negligible ionization, it is necessary to inquire as to whether there be some property of these particular flames which prevents ion formation with impurities present. To answer this question both lithium and sodium chloride solutions were sprayed into a carbon disulfide flame in the manner described above and the positive-ion concentration determined. The results from this experiment are recorded in table 3. Examination of these data indicates that there is no difference in ability of a carbon disulfide-air and a propane-air flame to ionize a salt which is present.

Since it has been demonstrated that two flames, those of carbon disulfide and hydrogen sulfide, do not afford ion concentrations comparable to that of propane, and since if ionization were due to contaminants these flames would be expected to have comparable ionization, it can be concluded that ionization in hydrocarbon flames is probably not due to contaminants but is a property of the flame.

## V. Ionization in Very Lean Flames

The ion concentration through the flame front has been determined for very lean propane-air flames burning on the flat-flame burner. Since the stability limits on such burners are very narrow, the equivalence ratio has been altered by the addition of nitrogen to the air. This has in addition made it possible to burn at an equivalence ratio of 0.835 (table 4) with a flame temperature of only 1535°K compared with the adiabatic flame temperature with undiluted air (at this same equivalence ratio) of 2080°K.

The ion concentrations at different positions in the flame front are presented in figure 9 for a series of equivalence ratios. The distances are determined relative to the position at which the tip of the probe just becomes red. This plane of reference was chosen rather than the visible cone because it is more definitive. At some future date this plane can be related to the position of the visible cone and to the measurements of temperature or of radical concentrations obtained by others. In general the edge of the visible cone on the unburned side occurs at zero. By means of the flow velocity the distance scale has been converted to time (fig. 10). This curve is only approximate on the unburned side because in order to correct the flow velocity the temperature profile was approximated from that obtained by Friedman (13). This profile is shown in figure 4 of the present paper. On the burned side the flow velocity was corrected for an increase in temperature to the adiabatic flame temperature. The ions are formed in the luminous cone and then disappear very rapidly by recombination. The ion concentration upstream from the luminous zone (zero) must be due either to diffusion ahead of the flame front or to perturbation of the flame by the probe.

It is of interest to compare these results with information obtained previously by deflection of a n-butane-air flame (equivalence ratio 0.8) in an electric field (1, 2). From a theory of the deflection based upon an electric wind concept it was deduced that the thickness of the ionization zone was 0.8 mm and the positive-ion concentration about  $10^{12}$  ions/cc. The thickness of

the ion zone reported in figure 12 is about 0.4 mm, and the observed ion concentration corrected to one atmosphere is  $1.8 \times 10^9$  ions/cc. Assuming that the ratio of actual to observed ion concentration is here the same as for salts added to the flame -- namely, 400 -- a true ion concentration of  $0.73 \times 10^{12}$  is obtained. The agreement is as good as one could expect and indicates the consistency of the several observations.

This set of probe data negates the possibility that ions result from thermal ionization of impurities in the input feed to the burner, such as atmospheric contamination by alkalis. The peak in the ionization curves (figs. 9 and 10) could not arise from contamination because the contaminant concentration would not drop off but would instead remain essentially constant, as does the temperature (fig. 4). To explain the peaks as being due to contaminants would require the assumption that ionization is due to a transfer of energy in collisions between chemi-activated species and the impurity. Moreover, to account for  $10^9$  ions/cc at 1400°K, assuming sodium as the contaminant, would require  $9.4 \times 10^{16}$  atoms of sodium/cc at 25°C. This is 0.3 mole-percent sodium contaminant in the input gases.

The possibility of nitric oxide as the ion species is also eliminated by these data because the thermodynamic equilibrium concentration of  $\text{NO}^+$  for these flames is less than one ion/cc.

#### VI. Effect of Equivalence Ratio on Ion Concentration

The effect on the ion concentration of varying the equivalence ratio was observed by probing inverted flames at 0.3 atmosphere. Inverted flames were chosen so that the flame could be approached with the probe from the unburned side at various equivalence ratios in the same apparatus. These flames were stabilized on a rod held in a laminar stream emanating from a rectangular duct (fig. 11). Very stable flames were obtained at 0.3 atmosphere but at other pressures slight oscillations made it difficult to probe the combustion

zone. The distance the probe moved into the burning zone was corrected for the angle between the probe and the flame.

The results for lean flames are reported in figure 12 and for rich flames in figure 13. The thickness of the ionized region has been increased by a reduction in pressure (cf. fig. 9) just as the thickness of the luminous zone is increased by a reduction in pressure. In figure 14 the maximum observed positive-ion concentration is plotted against the equivalence ratio along with the adiabatic flame temperature and the burning velocity. All three curves have the same general shape except that the burning velocity drops off considerably faster on the rich side than does the flame temperature or the ion concentration. At any given temperature the ion concentration on the rich side is slightly greater than on the lean side but not sufficiently to make a strong argument for carbon particles as the ion source (5, 8). Neither does this result eliminate the possibility that the ions are polymerized carbon.

If Saha's equation be rewritten,

$$2 \log N_+ - \frac{3}{2} \log T = (\log N_0 + \log G + 15.38) - \frac{5040}{T} V_i$$

it is seen to be possible from a plot of  $\log (N_+^2/T^{3/2})$  against  $1/T$  to calculate the ionization potential,  $V_i$ , and the concentration of un-ionized species, provided the species being ionized remains constant throughout the range of composition. This would approximate the situation if the ions were due to contaminants. The results at one atmosphere with nitrogen dilution (table 4) have been corrected to 0.3 atmosphere, assuming Saha's equation to apply, which gives  $N_+(0.3 \text{ atm}) = N_+(1 \text{ atm}) \sqrt{0.3}$ .

The function  $\log (N_+^2/T^{3/2})$  is plotted against the reciprocal of the adiabatic flame temperature in figure 15. The points for 0.3 atmosphere, banded by dotted lines, show considerable scatter but are definitely not in

the same region as the data obtained at one atmosphere. This is further evidence that the ions are not due to contaminants because the points would then lie on the same curve.

### Summary and Conclusions

In addition to an indication of the usefulness within limits of the Langmuir probe for studying ionization in flames, the main conclusion to be drawn from this paper is that ionization in the combustion wave of hydrocarbon flames is not due to thermal ionization of contaminants or nitric oxide. The arguments presented for this conclusion are:

1. Flames of carbon disulfide and hydrogen sulfide contain very small concentrations of ions. Were contaminants responsible, these flames would be expected to afford ion concentrations comparable to hydrocarbon flames.
2. Very lean flames at low temperatures have high ion concentrations.
  - a. Close to one mole-percent sodium impurity in the input gas would be required to account for the observed concentration.
  - b. The thermodynamic concentration of  $\text{NO}^+$  in these flames is less than one ion/cc.
3. The ionization is concentrated in a very thin region comparable in thickness to the reaction zone.
4. One cannot correlate the results at two pressures by assuming thermal ionization of contaminants.

### References

1. Calcote, H. F.: Third Symposium on Combustion, Flame and Explosion Phenomena, p. 245. Baltimore, The Williams and Wilkins Company (1949).
2. Calcote, H. F., and Pease, R. N.: Ind. Eng. Chem., 43, 2726 (1951).
3. Langmuir, I., and Mott-Smith, H. M.: Gen. Elec. Rev., 25, 731 (1923); 27, 449, 583, 616, 726, 810 (1924).
4. Belcher, H., and Sugden, T. M.: Proc. Roy. Soc. London, 201, 480; 202, 17 (1950).
5. Shuler, K. E., and Weber, J.: J. Chem. Phys., 22, 491-502 (1954).
6. Taylor, H. S., and Glasstone, S.: A Treatise on Physical Chemistry, p. 388. N. Y., D. Van Nostrand Co. (1943).
7. Gaydon, A. G., and Wolfhard, H. G.: Flames, Their Structure, Radiation and Temperature, Chapter 13. London, Chapman and Hall (1953).
8. Lewis, B., and Von Elbe, G.: Combustion, Flames and Explosions of Gases, p. 206. New York, Academic Press (1951).
9. Moyerman, R. M., and Shuler, K. E.: Science, 118, 612-614 (1953).
10. Wilson, H. A.: Rev. Mod. Phys., 3, 156 (1931).
11. Loeb, L. B.: Fundamental Processes of Electrical Discharge in Gases. N. Y., J. Wiley and Sons (1939).
12. Glasstone, S., Laidler, K. J., and Eyring, H.: The Theory of Rate Processes. N. Y., McGraw-Hill (1941).
13. Firedman, R.: Fourth Symposium on Combustion, p. 259. Baltimore, The Williams and Wilkins Company (1953).

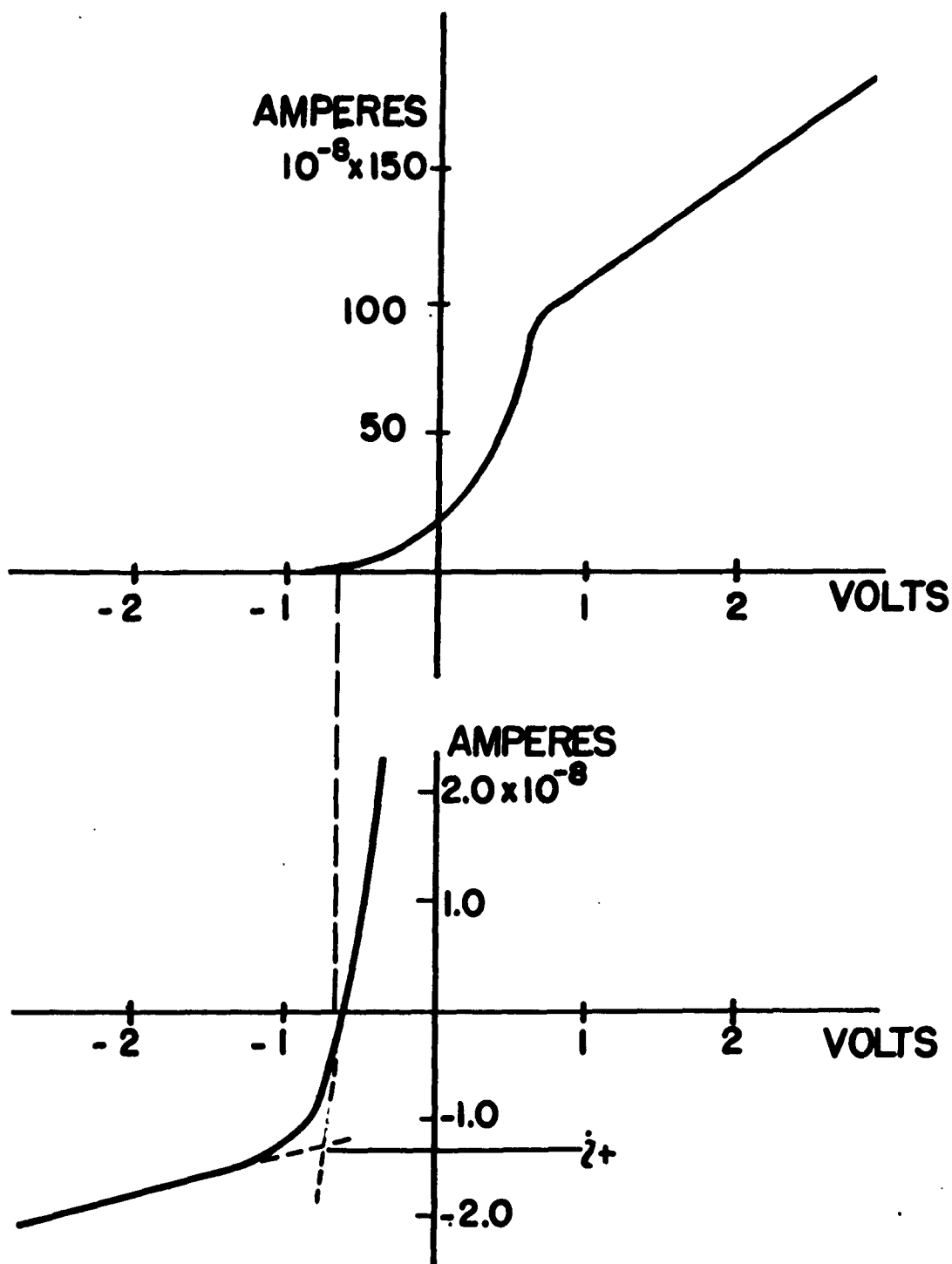


FIGURE 1. Typical forward probe curves. Electron current to probe point is the positive direction.



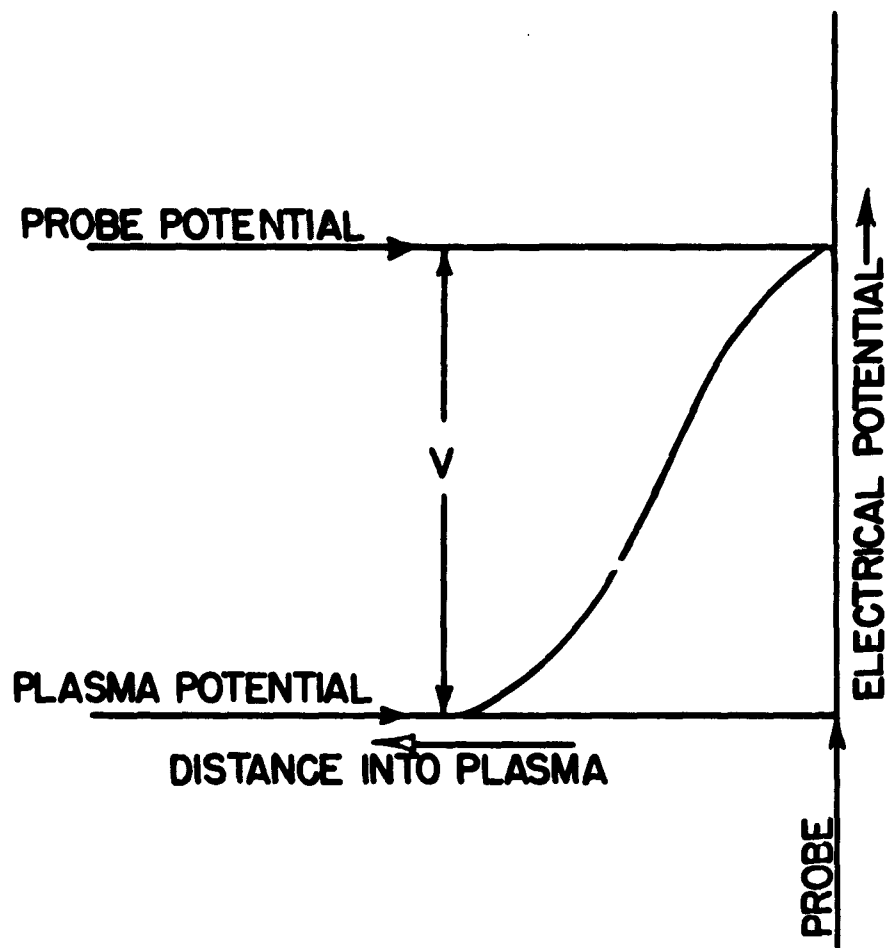


FIGURE 1. PROBE POTENTIAL PROFILE IN A PLASMA  
WITH A PROBE OF FINITE SIZE.

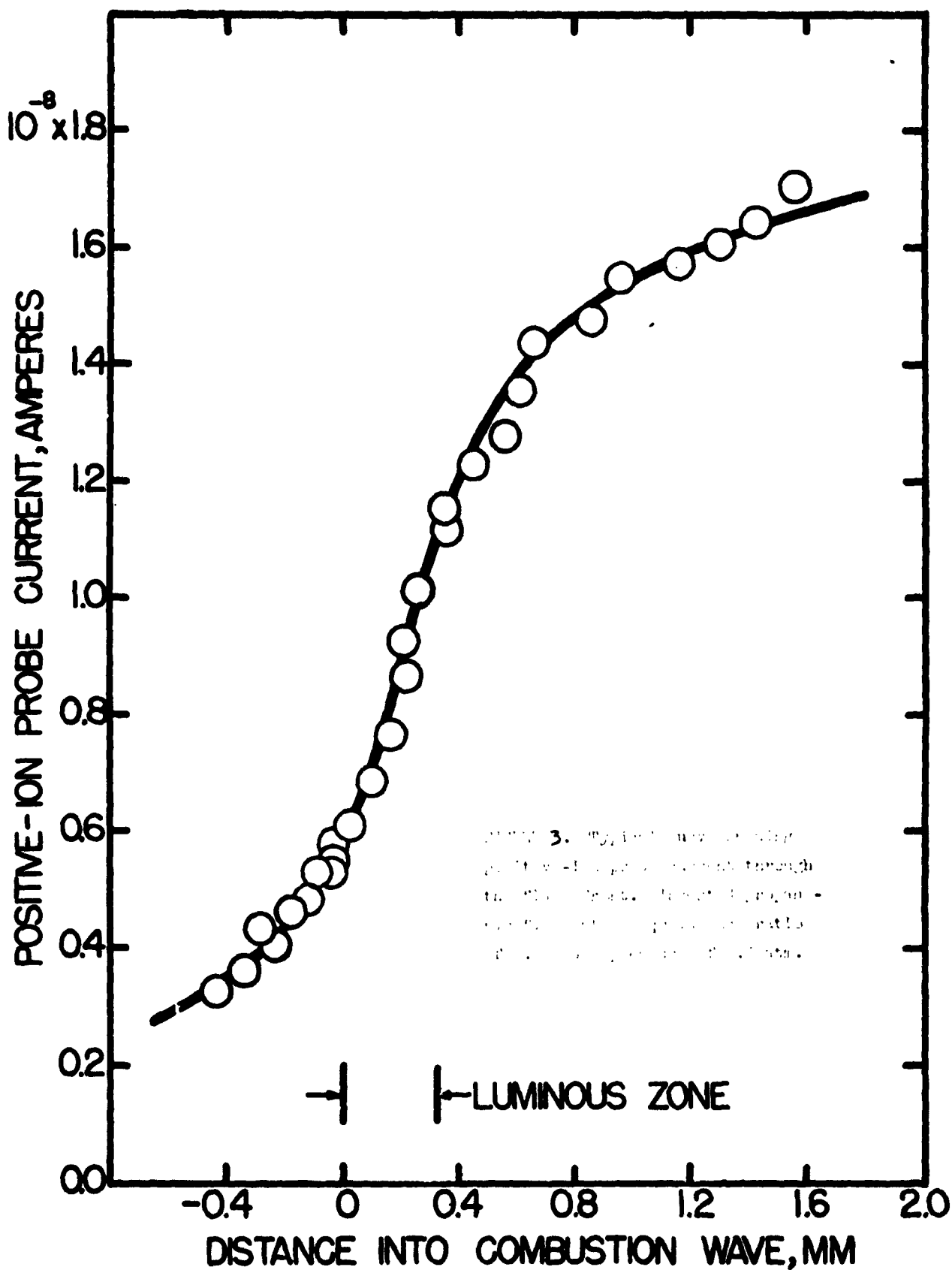


FIGURE 4. Typical curves showing positive-ion concentration and temperature through the flame front. Propane-air flame at an equivalence ratio of 0.8. Ion-concentration curve at 0.3 atm using inverted flame. Temperature curve at 0.975 atm on flat-flame burner (13).

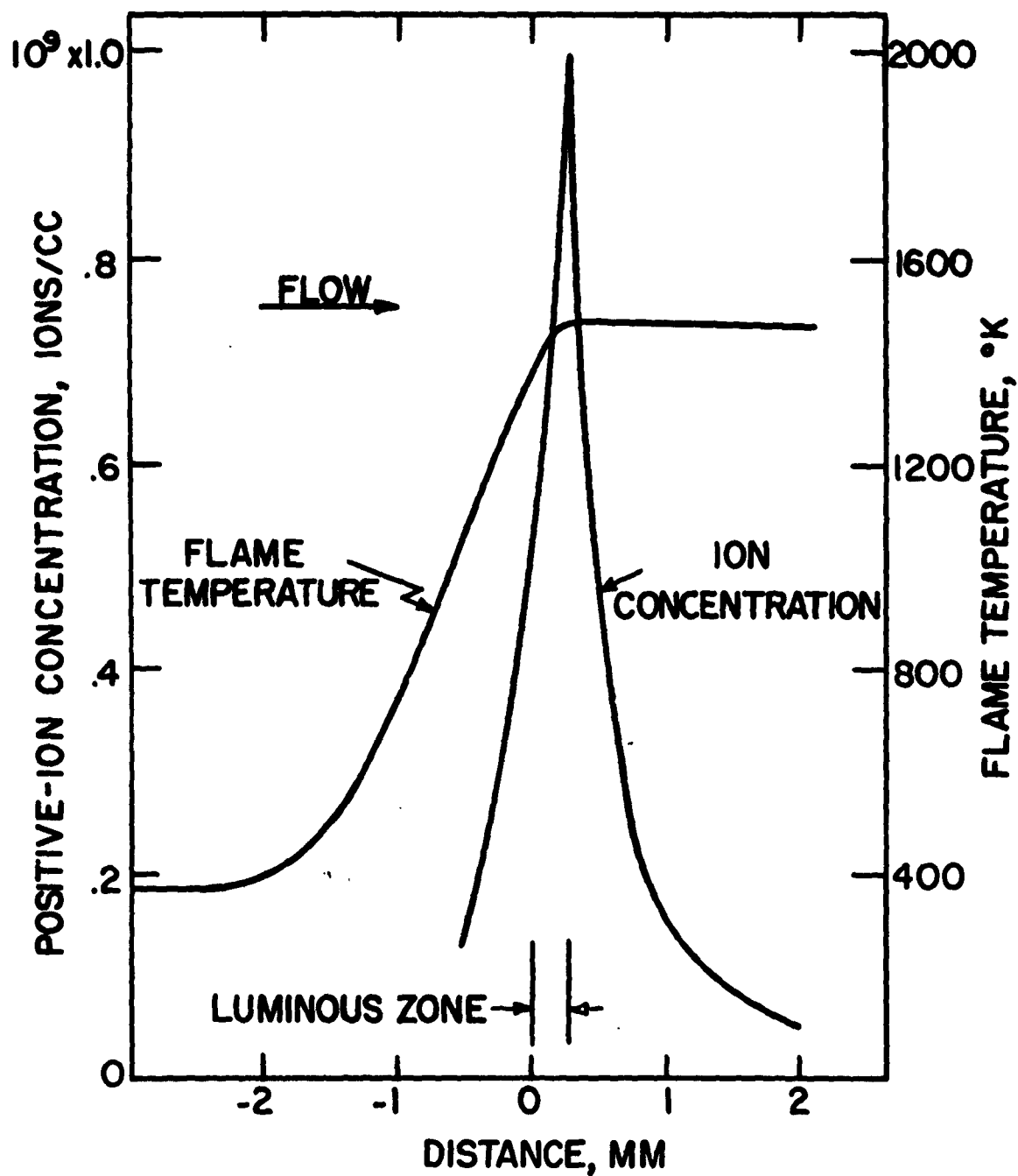
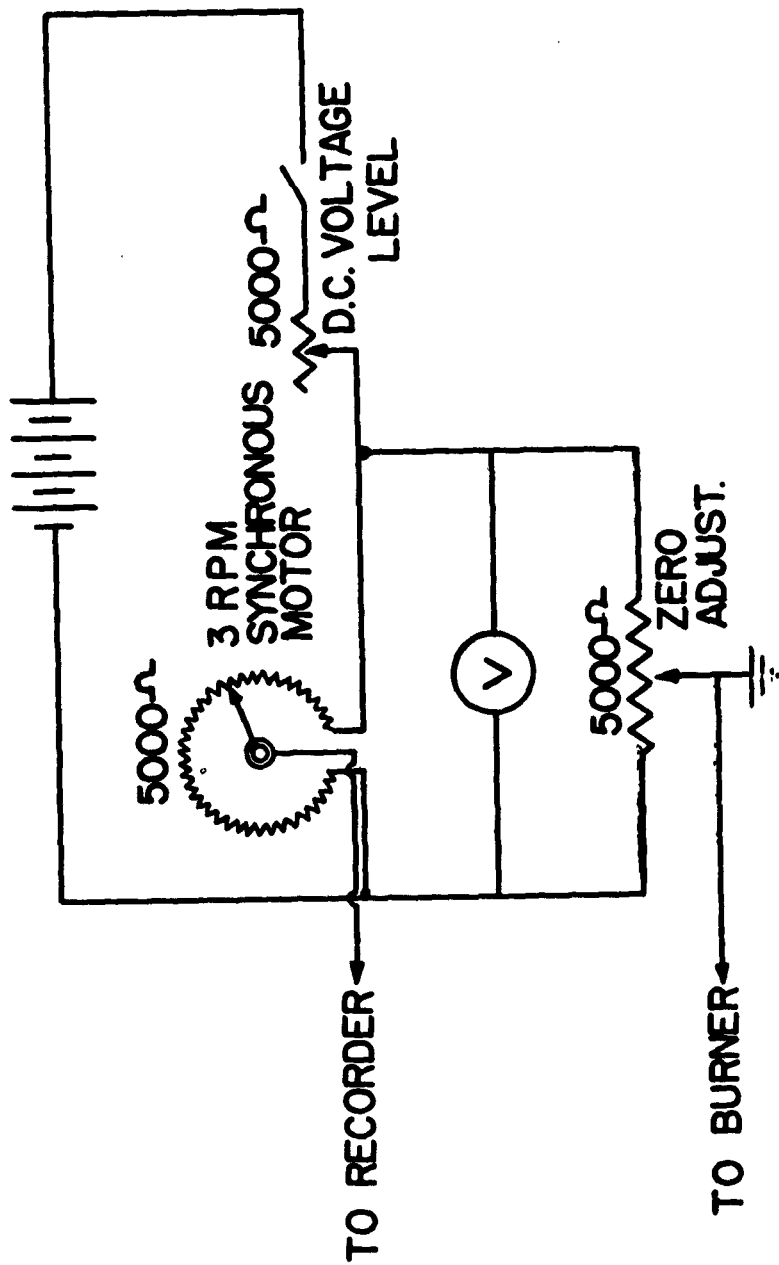


FIGURE 5. Variable-voltage supply unit for burner calibration.



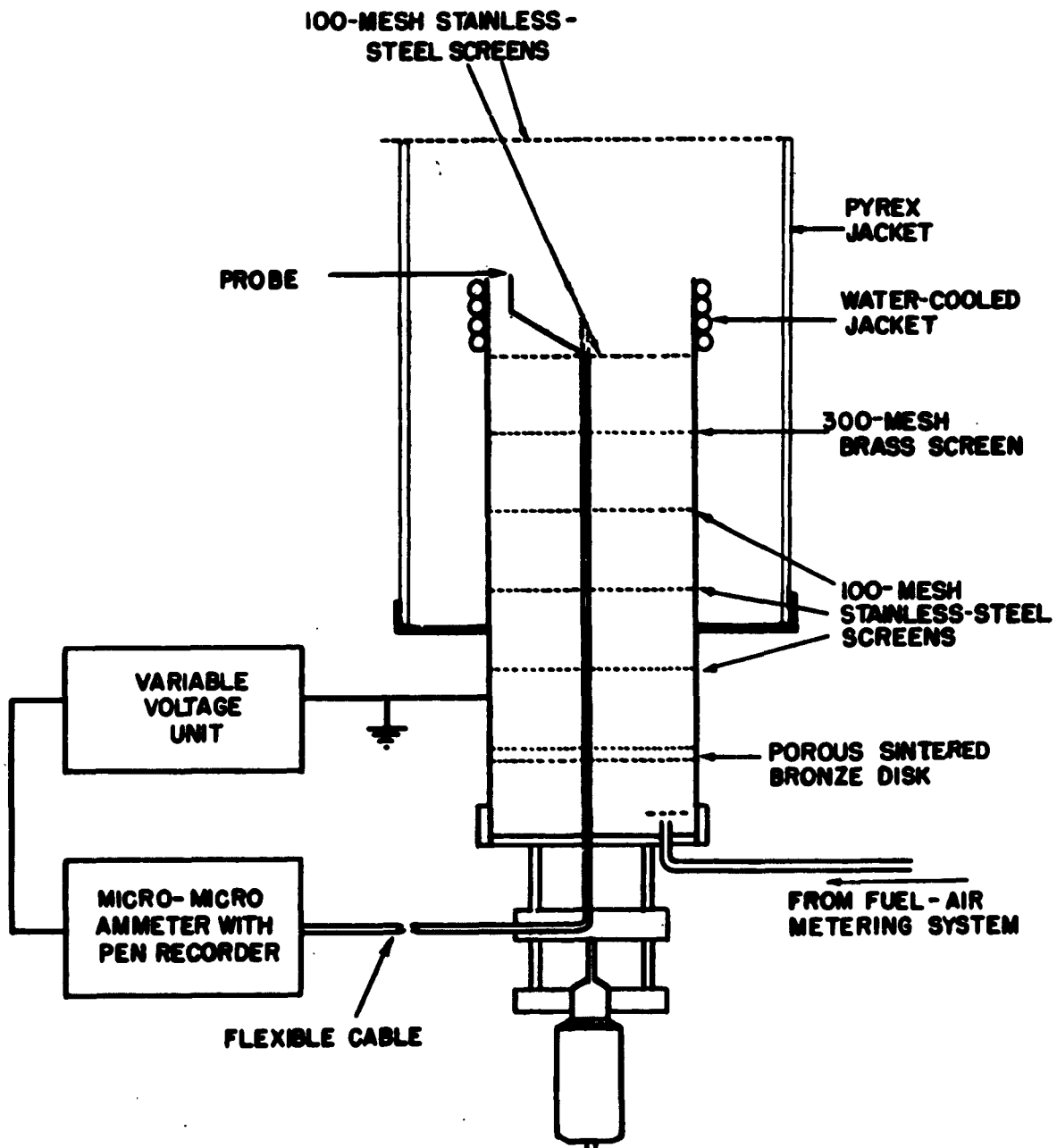


FIGURE 6. Flat-flame burner and probe circuits.

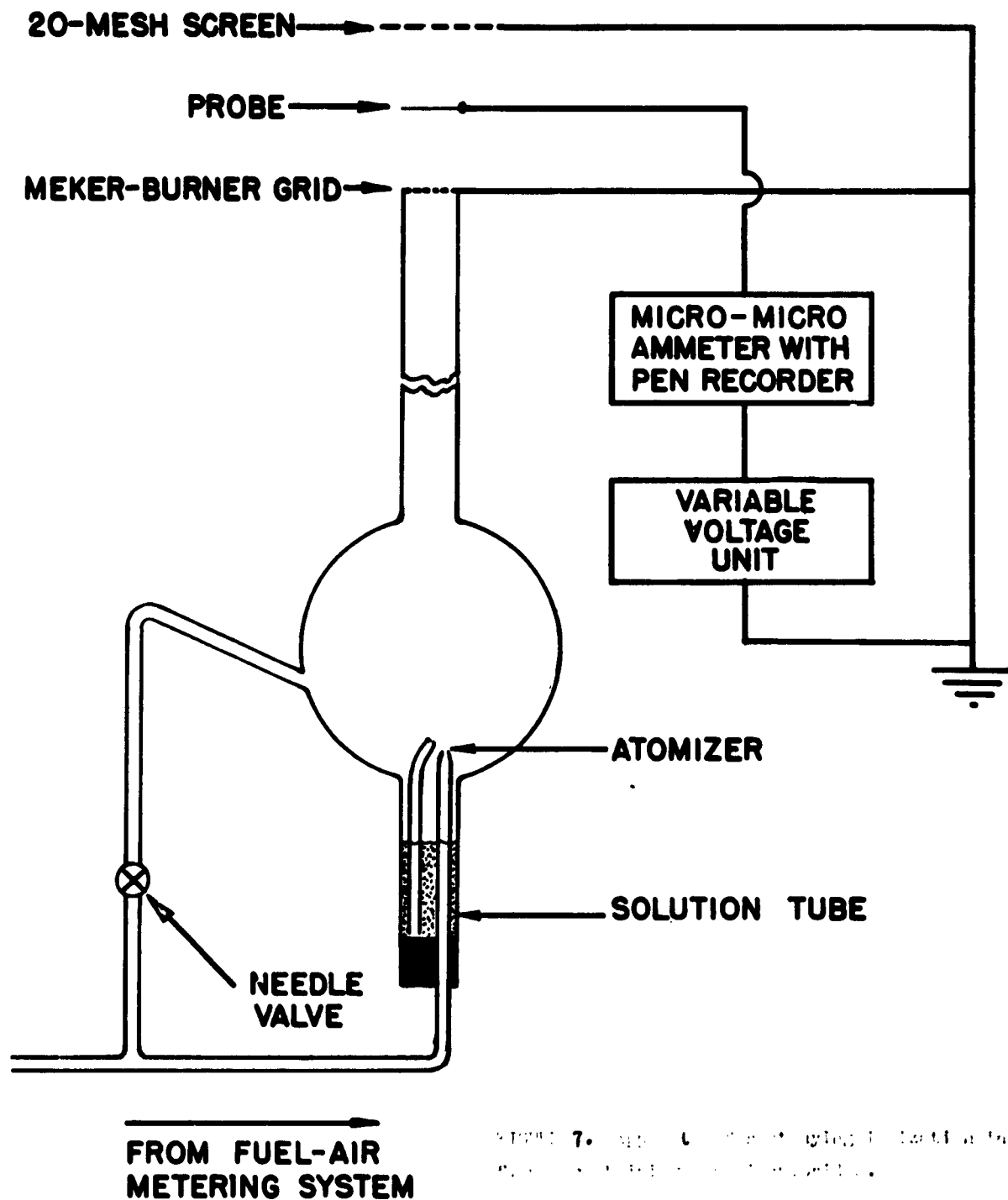
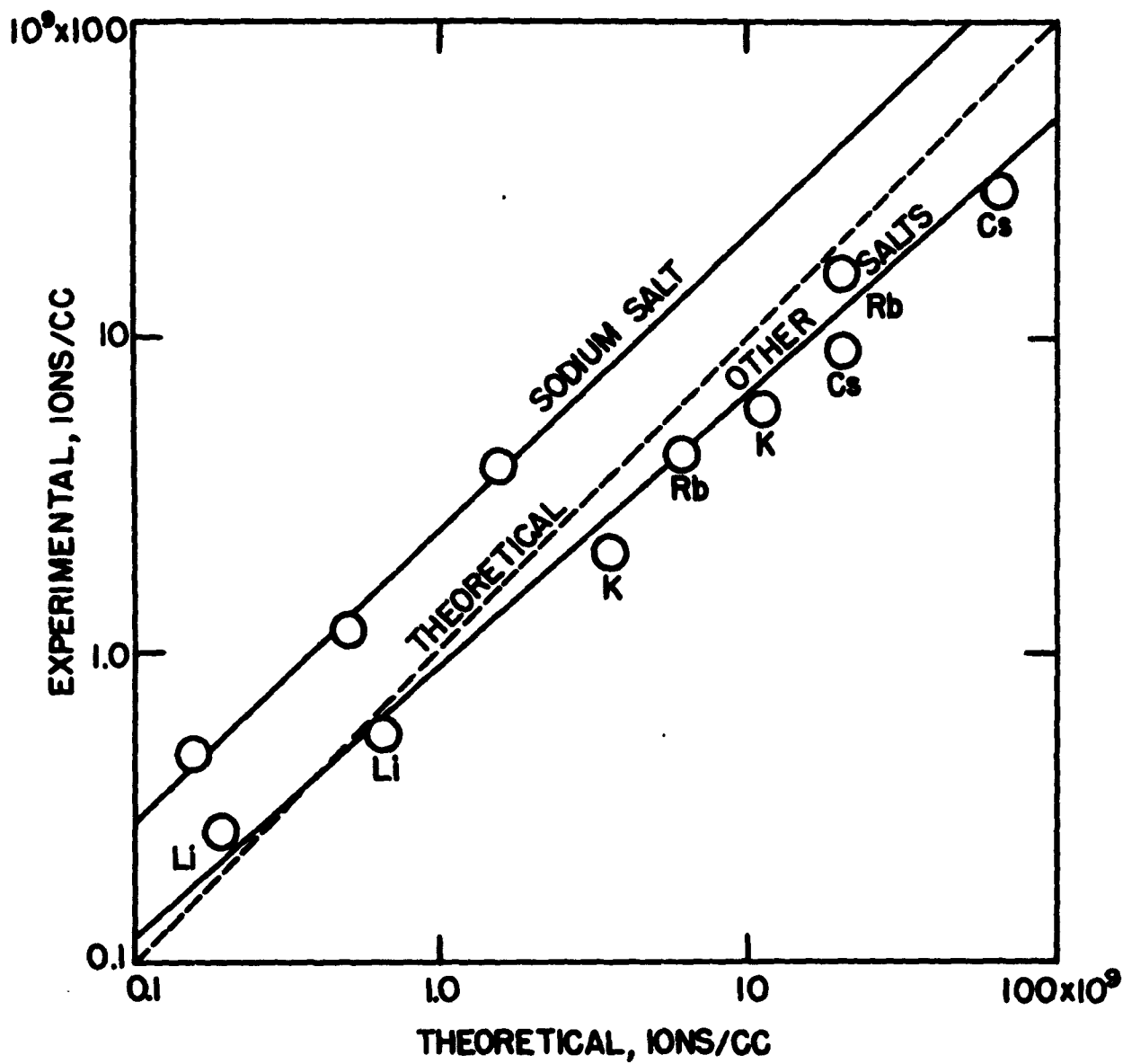


FIGURE 7. Probe atomization system for electrochemical analysis.

FIGURE 8. Experimental and theoretical positive-ion concentrations for propane-air flames containing alkali chlorides at an assumed equilibrium temperature of 1500°K.



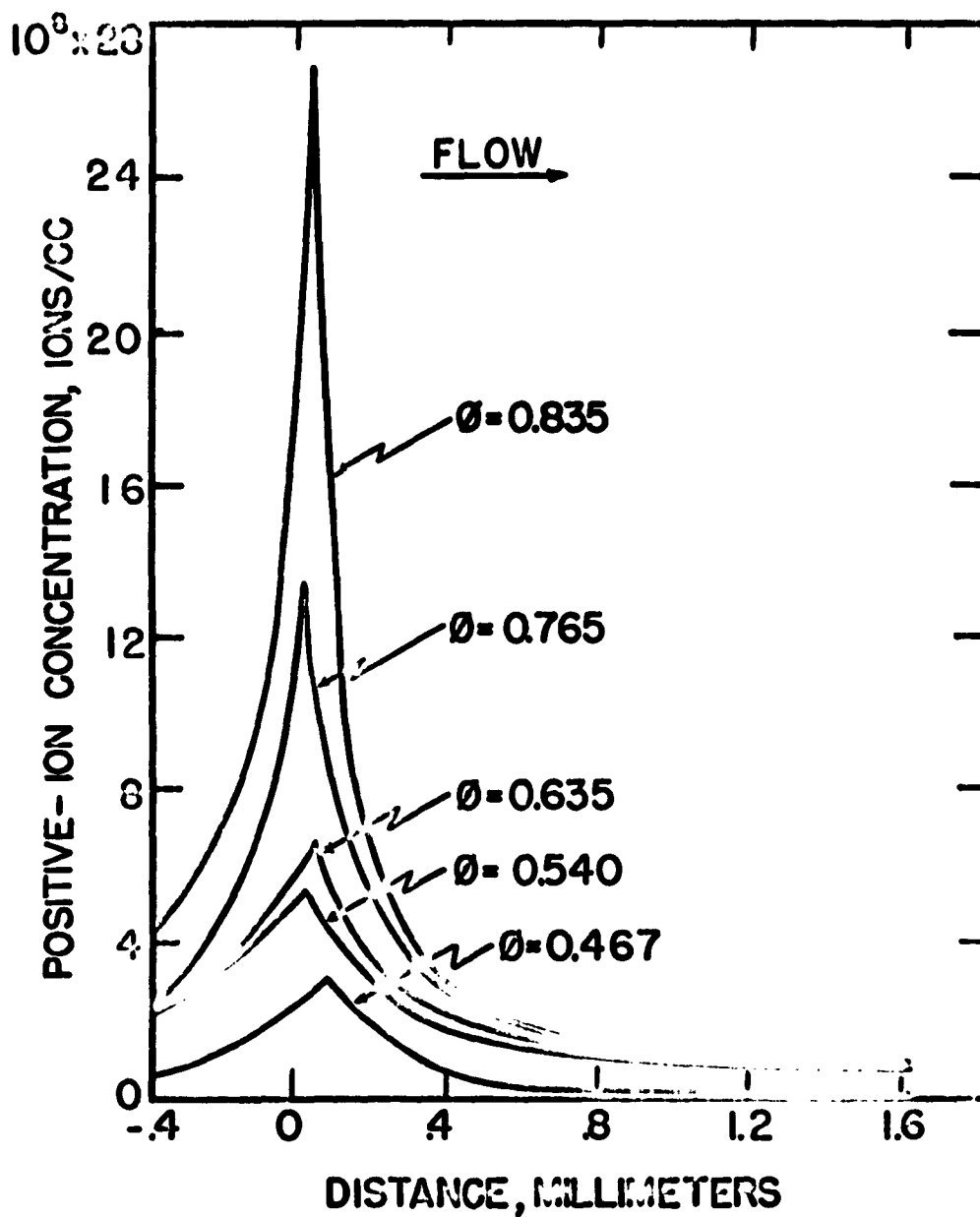


FIGURE 9. Positive-ion concentration through the flow channel as a function of distance. Applied voltage = 10 kV, flow rate = 100 cc/min. Plot of  $\theta$  versus distance is shown in Figure 10.



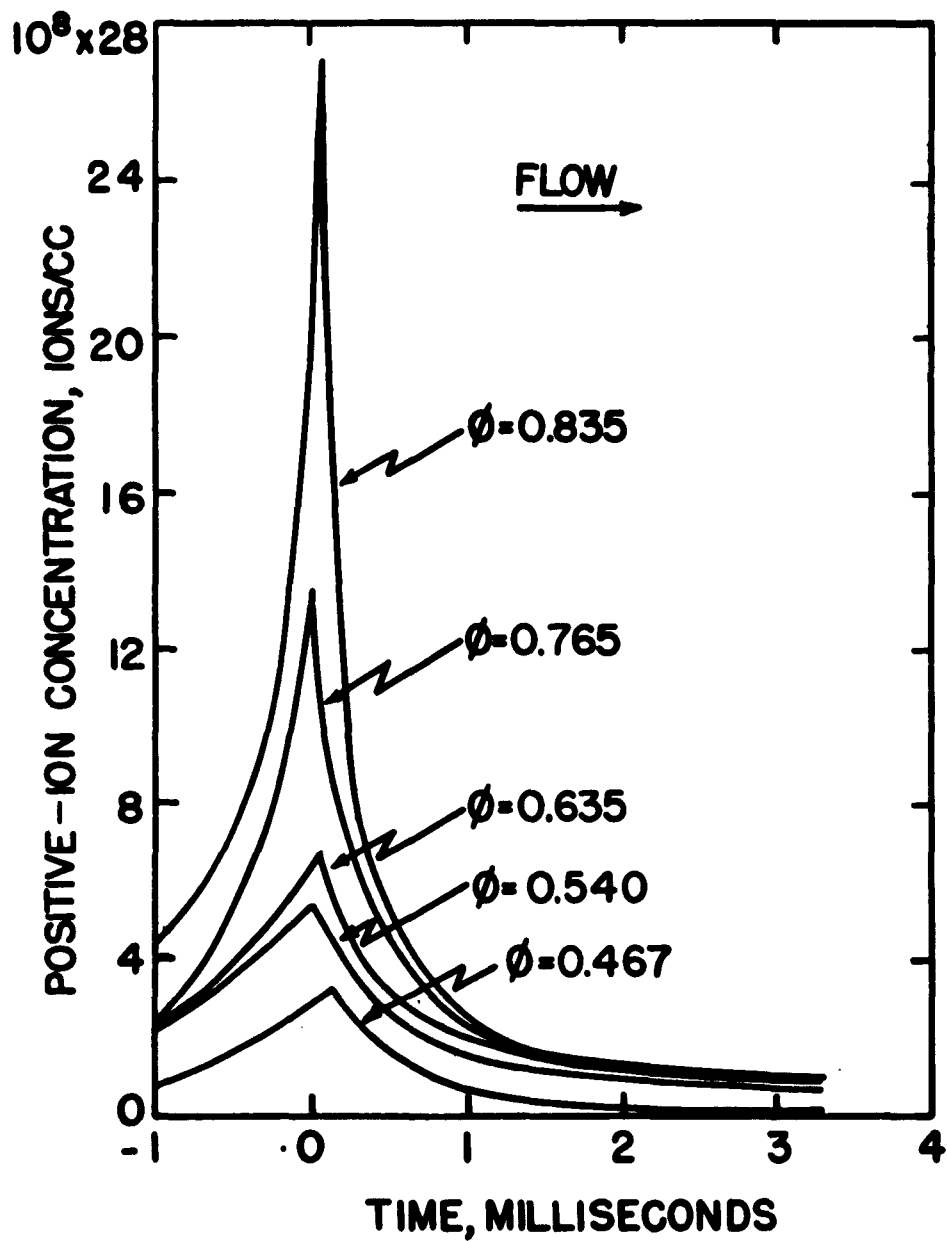


FIGURE 10. Positive-ion concentration through the flame front as a function of time. Equivalence ratio varied by diluting air with nitrogen. Flat-flame burner at one atmosphere.

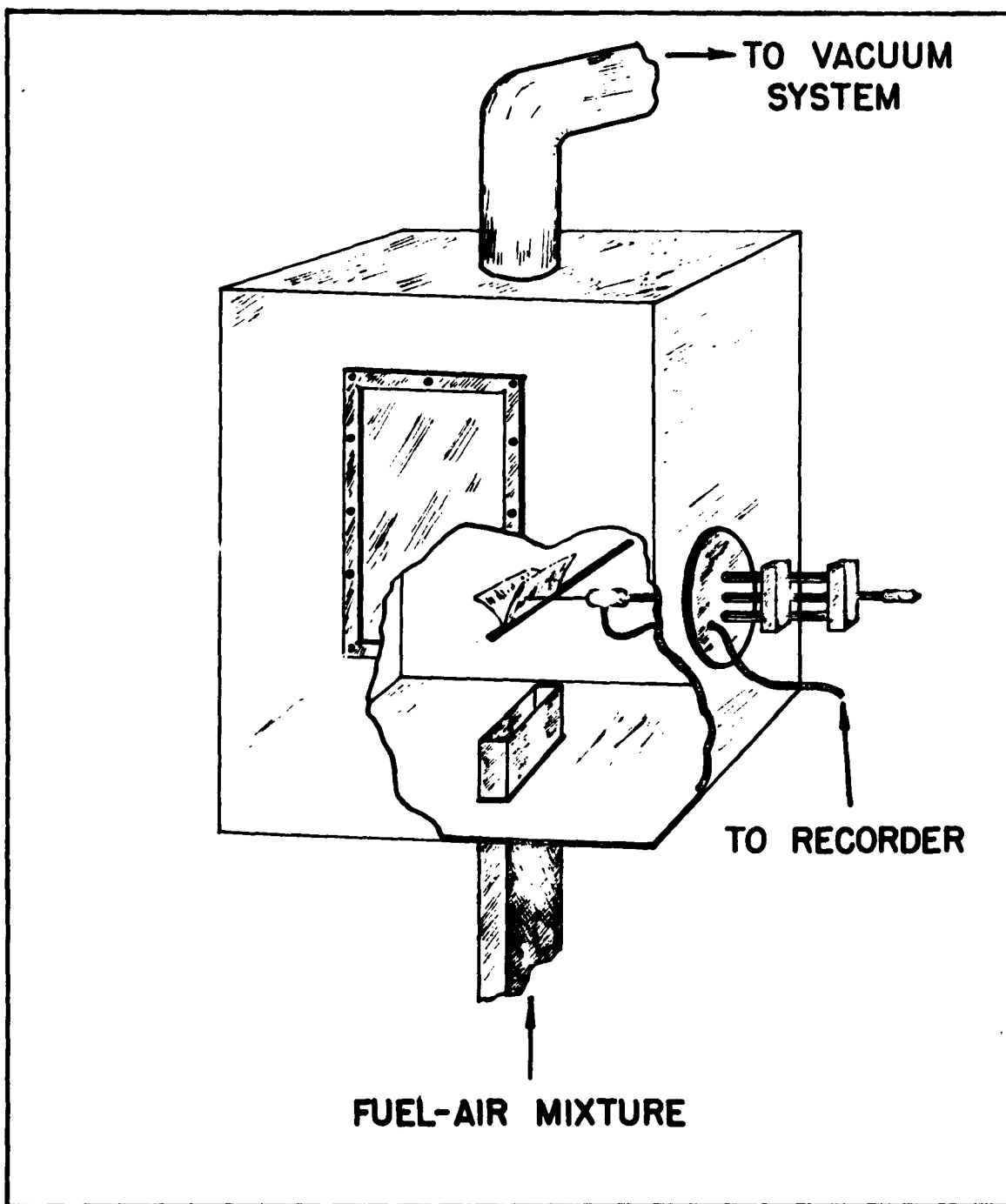


FIGURE 11. Inverted flame at constant speed apparatus.

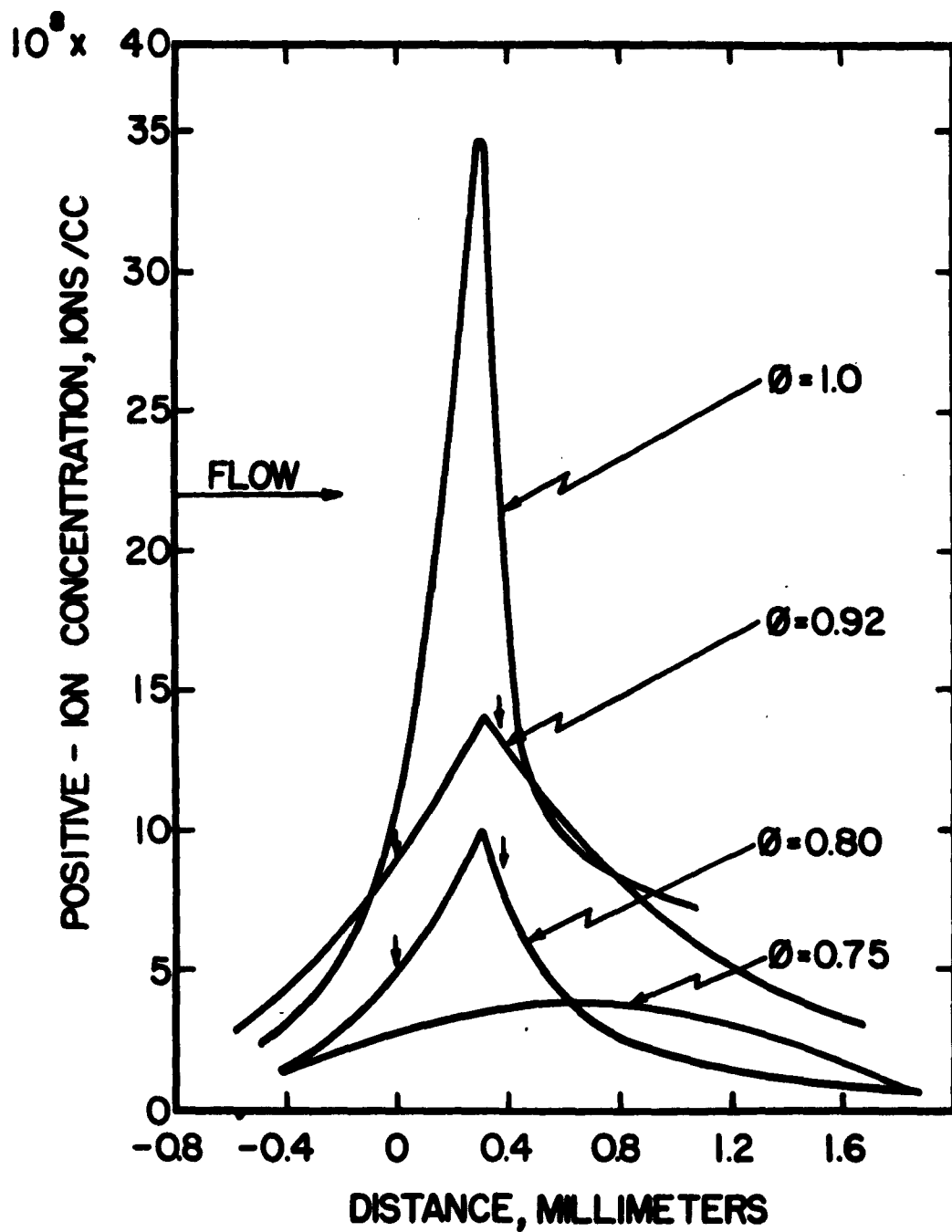


FIGURE 12. Positive-ion concentration through the flame front. Inverted propane-air flame at 0.5 atmosphere. Arrows indicate extent of luminous zone.

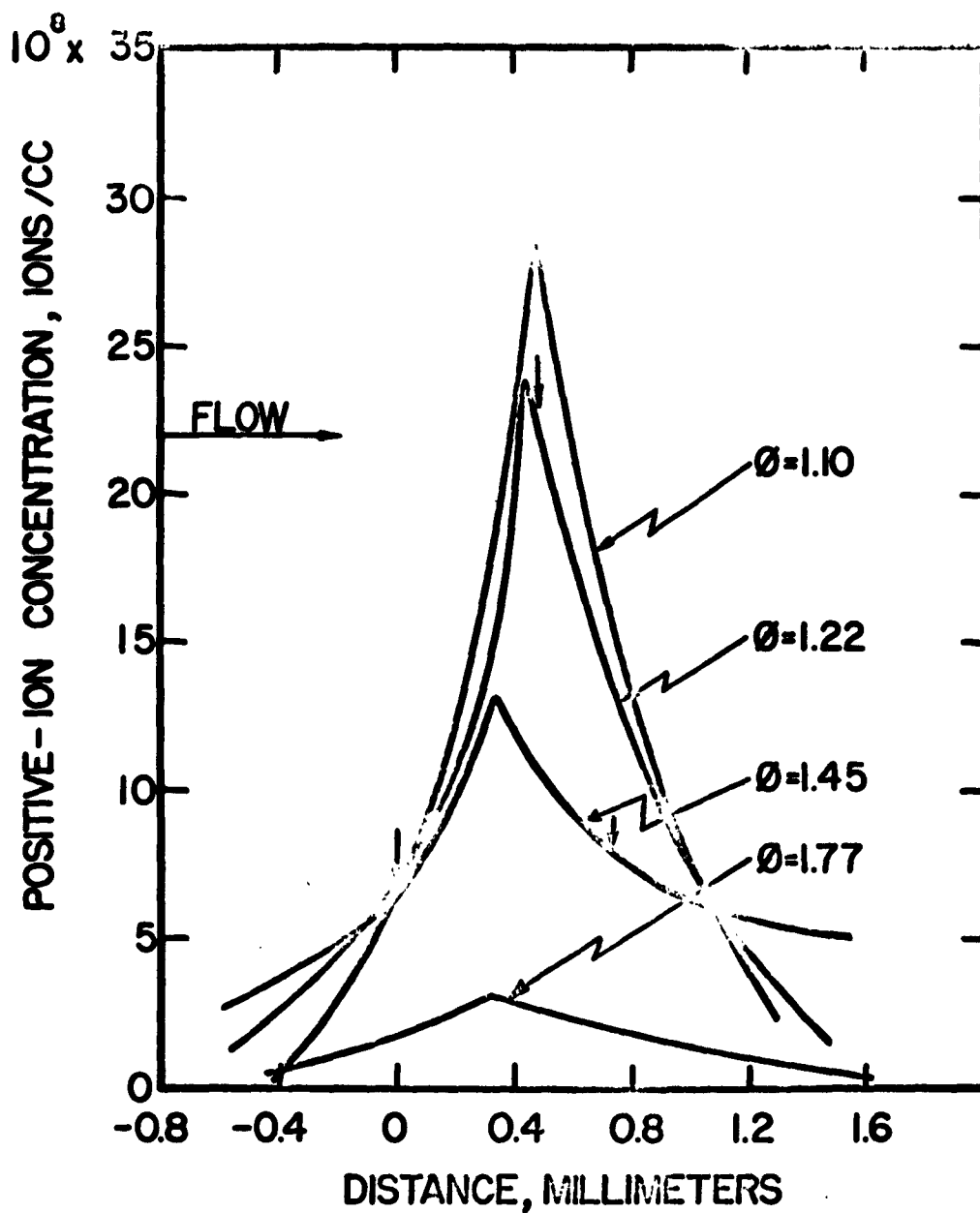
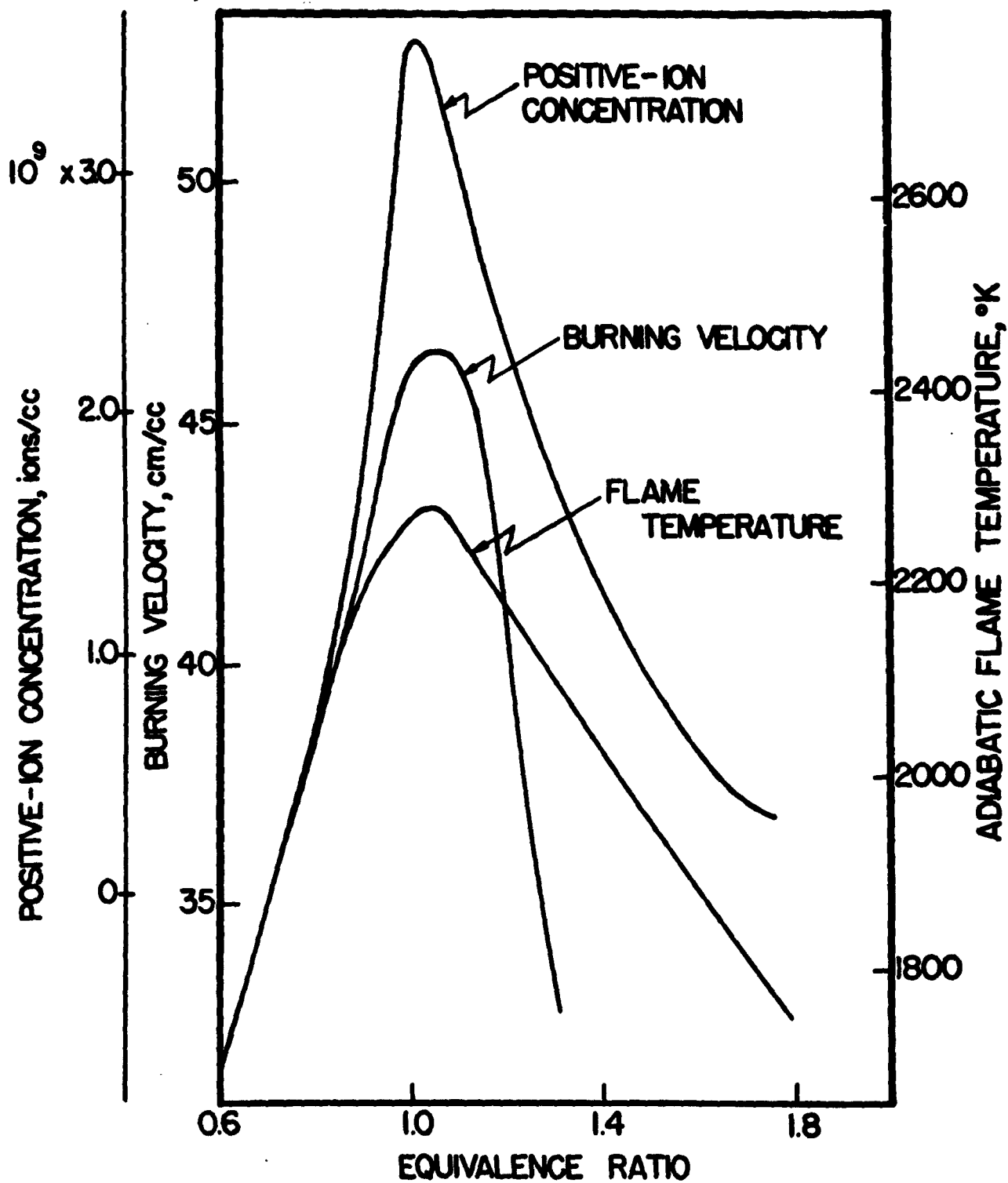


FIG. 1. Positive-ion concentration in the flow front, plotted against distance from the flow front. Arrows indicate extent of bubble trail.

FIGURE 14. Positive-ion concentration (0.5 atmosphere), burning velocity (1.0 atmosphere), and flame temperature as functions of equivalence ratio.



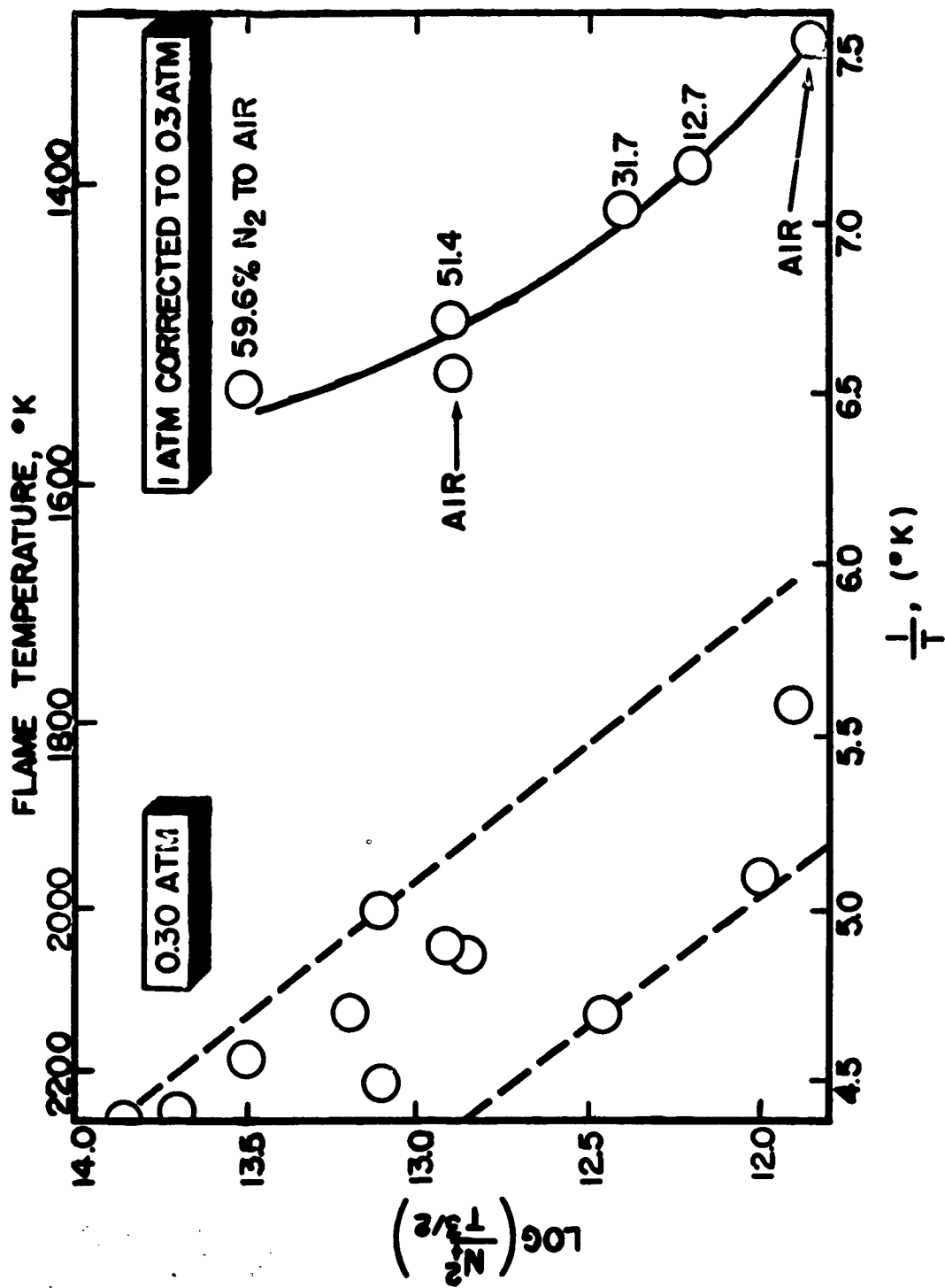


FIGURE 10. Designated temperature conditions of Table 1.  
 (Values are corrected to 0.30 ATM.)